

## Excessive Iron and Weightlessness Effects on the Femurs and Livers of Rats

Aidong Wang; Jiachen Zang; Jing Wang; Guangjun Nie; Guanghua Zhao; Bin Chen

- BACKGROUND:** Weightlessness results in negative physiological changes. Excessive iron in organisms likewise leads to numerous damages. In this study, we investigated the effect of a combination of iron overload and weightlessness simulated by tail-suspending on rats.
- METHODS:** Male Wistar rats were randomly divided into four groups: control (CON), iron overload (IO), simulated weightlessness (SW), and iron overload plus simulated weightlessness (IO+SW). After the experiment, the rats were evaluated through routine blood, serum ferritin, histology, and micro-computed tomography analyses.
- RESULTS:** As compared to CON, a combination of IO and SW resulted in a 15.9% loss of rat bodyweight versus treatment with each alone (3.3% in IO, 11.7% in SW group). Although iron overload is mainly responsible for an increase in hemoglobin (4.7% in IO the group) and serum ferritin (71.7% in IO group) concentration, simulated weightlessness facilitates such increase (5.3% and 118.4% in IO + SW group, respectively). Similarly, iron overload resulted in severe iron deposition on the liver and spleen, and the deposition became more serious in the combined model. In contrast, the simulated weightlessness is mainly responsible for the damage to the femur.
- DISCUSSION:** All the results demonstrated that the combined conditions exhibited a significantly different effect on rats from those with either simulated weightlessness or iron overload alone, and that these different effects are organ-dependent.
- KEYWORDS:** bodyweight, liver, bone, hepcidin.

Wang A, Zang J, Wang J, Nie G, Zhao G, Chen B. *Excessive iron and weightlessness effects on the femurs and livers of rats*. *Aerosp Med Hum Perform*. 2015; 86(1):8–14.

The effects of weightlessness or microgravity in space are an ongoing issue. Numerous studies characterizing the negative effects of weightlessness mainly on bone, calcium balance, muscle mass, cephalic fluid, and the immune system have been reported.<sup>2</sup> Among these effects, bone loss has received more attention due to its serious consequences, particularly for space travel of longer durations,<sup>1</sup> which is the future direction of spaceflight. Also, a long-term increase in tissue iron availability and storage during spaceflight is cause for concern and represents a potential general risk across all performance and disease conditions in space.<sup>18</sup> Namely, weightlessness during long-duration spaceflight is one of the unusual stimulations that induces iron overload. Normally, hereditary iron overload is mainly caused by mutations in the iron metabolism genes (HFE, HJV, HAMP, TFR2, and SLC40A1),<sup>3</sup> while secondary iron overload is often associated with many commonly known conditions such as the high consumption of iron-rich food, inappropriate supplementation of iron, accumulation of iron in vivo caused by severe anemia, and the necessity of transfusion in some patients.<sup>25</sup>

Being a component of numerous biological enzymes and metalloproteins makes iron ubiquitous in cells and essential for life. Since iron is involved in many critical physiological processes, the homeostasis maintained by the balance between iron use, absorption, storage, and recycling is vitally important.<sup>19</sup> An excessive amount of free iron is deleterious, because iron can lead to reactive oxygen species, which can chemically attack macromolecules, including deoxyribonucleic acid, proteins, and lipids.<sup>8</sup>

From the CAU & ACC Joint-Laboratory of Space Food, College of Food Science and Nutritional Engineering, China Agricultural University, Key Laboratory of Functional Dairy, Ministry of Education, Beijing, China; the Key Laboratory of Space Nutrition and Food Engineering, China Astronaut Research and Training Center, Beijing, China; and the Chinese Academy of Sciences Key Laboratory for Biomedical Effects of Nanomaterials and Nanosafety, National Center for Nanosciences and Technology of China, Beijing, China.

This manuscript was received for review in May 2014. It was accepted for publication in September 2014.

Address correspondence to: Guanghua Zhao, Mailbox 303, 17 Qinghaudonglu, Haidian District, Beijing 100083, China; gzha@cau.edu.cn; or Bin Chen, China Astronaut Research and Training Center, Haidian District, Beijing 100094, China; chenb12@yahoo.com.cn.

Reprint & Copyright © by the Aerospace Medical Association, Alexandria, VA.

DOI: 10.3357/AMHP.4074.2015

There is a complex system that exists in the human body to fulfill the metabolic demand for iron and to maintain physiological concentrations in the plasma compartment and different organs. In this system, hepcidin is a key regulator.<sup>9</sup> Hepcidin is a hepatocyte-produced peptide hormone that down regulates iron concentration by binding to and consequently inducing the internalization and degradation of the ferroportin protein.<sup>24</sup> Ferroportin is the only known transporter that exports iron from cells, making it possible to transfer iron from one cell type to another. Moreover, the secretion of hepcidin is in response to both iron loading and inflammation,<sup>15</sup> so an increase in hepcidin concentration in serum could be an indicator of iron overload in an organism.

The adverse effects of weightlessness and iron overload have been widely reported.<sup>2,8</sup> However, to the best of our knowledge, so far there has not yet been any report on the combined effect of iron overload and weightlessness on animals or humans. Therefore, the purpose of the present study was to evaluate the effect of a combination of iron overload and weightlessness simulated by tail-suspension of rats. Fe-dextran treatment, that leads to similar pathological and clinical consequences observed after acute iron overload in humans, constitutes a good model for iron toxicity assessment.<sup>16</sup> Weightlessness simulated by tail-suspension, as described by NASA, is technically appropriate<sup>13</sup> and widely used in microgravity models.

## METHODS

### Animals

Animals were handled and treated in accordance with the Regulations for the Administration of Affairs Concerning Experimental Animals (Approved by the State Council of P.R. China, 1988). All the procedures were approved by the Institutional Animal Ethical Committee of the China Agricultural University.

Forty male Wistar rats at 7 wk of age (Experimental Animal Center of Military Medical Sciences, Beijing, China), with 220–235 g of bodyweight, were group housed and allowed to acclimate to the environment for 7 d on a 12-h light/dark cycle and constant relative humidity of 55% at  $25 \pm 2^\circ\text{C}$ . All the animals were given free access to commercial animal chow (Experimental Animal Center of Military Medical Sciences, Beijing, China) and water. After acclimation, rats were randomly divided into control (CON), iron overload (IO), simulated weightlessness (SW), and iron overload and simulated weightlessness (IO+SW) groups, and were housed alone in specially designed cages with bodyweights being recorded every 3 d. Rats in the SW and IO+SW groups were tail-suspended for 24 d while, in the other two groups, the rats were caged individually without tail suspension under the same condition. Rats in IO and IO+SW groups were given five doses (one dose every 2 d) intraperitoneal injection of iron-dextran at a dose of  $100 \text{ mg} \cdot \text{kg}^{-1}$  bodyweight while, correspondingly, the other two groups received an isovolumic injection of saline.

### Equipment

Weightlessness was simulated using a modified version of the tail suspension technique.<sup>13</sup> A strip of elastic hairpin loop secured by strips of the tape on the cleaned tail and a link chain preattached to the overhead bar of the cage was used to maintain the rat in about a  $30^\circ$  head-down tilt position with their hind limbs unloaded. Rotation of  $360^\circ$  and free access to food and water were allowed. Routine blood chemistry parameters were examined with an automated analyzer (Kohden, Tokyo, Japan). Serum ferritin was detected with a rat ferritin kit (IBL, Hamburg, Germany). Tissue sections were cut with a Microm HM 315 (Microm HM 315, Microm, Walldorf, Germany) microtome. Pathological evaluation and iron deposition analyses were examined using Image Plus (Rockville, MD). Micro-CT analyses were performed using  $\mu\text{CT}40$ , Scanco Medical, Brüttsellen, Switzerland. Relative concentrations of serum hepcidin were measured using matrix-assisted laser desorption/ionization time of flight mass spectrometry (Billerica, MA) analyses.

### Procedure

Animals were fasted overnight before sacrifice and then anesthetized with ethyl ether. Blood samples were quickly collected and part of the serum of every sample was separated for routine blood chemistry examination and serum ferritin analyses, respectively. The liver, heart, spleen, kidney, musculus gastrocnemius, and duodenum were carefully removed, fixed in 4% paraformaldehyde and 10% formalin solution, and then embedded in paraffin. Sections ( $\sim 5 \mu\text{m}$ ) were cut with the microtome and then stained with hematoxylin-eosin and Prussian blue for pathologic evaluation and iron deposition analyses, respectively.

Densitometric and morphometric micro-CT analyses were performed on the cortical bone and trabecular bone at the left distal femurs. Bones were scanned *ex vivo* using a micro-CT system. The energy settings were 55 kV and 145 mA, and at a  $32 \mu\text{m}$  voxel size. The processing system was used to firstly define cortical and trabecular regions of interest (ROIs) on all volumes. The ROIs extended from the region of the distal femur beginning at the growth plate proximally along the femur diaphysis for more than 1.7 mm. Trabecular ROIs were drawn free-hand on sequential slices, including the endosteal envelope, conforming to the endosteal contour on each slice. Cortical ROIs were defined as 1.7-mm segments of the mid-diaphysis of the femurs and resulted from digital subtraction of the respective trabecular ROIs from the whole bone volume.<sup>20</sup> All trabecular bone from each selected slice was segmented for three-dimensional reconstruction ( $\sigma = 1.2$ , supports = 2, and threshold = 180) to calculate the following parameters: bone mineral density, bone volume/total volume fraction (BV/TV), trabecular number (Tb.N), trabecular thickness (Tb.Th), trabecular separation (Tb.Sp), connectivity density, and structure model index.<sup>23</sup> The relative concentration of hepcidin in serum was measured using a modified version of a newly designed method depending on mesoporous silica chip enrichment and Maldi-TOF MS analysis.<sup>4</sup>

### Statistical Analysis

SPSS Statistics 19.0 was utilized to analyze the data. The difference between two groups was determined using the Student-Newman-Keul test. Also, the mean difference among groups compared with the control was determined by applying a one-way ANOVA followed by Dunnett's test. Data are shown in mean  $\pm$  SD and  $p < 0.05$  was considered statistically significant.

## RESULTS

Body growth [ $F(3, 36) = 25.594, p < 0.001$ ] was markedly reduced in the SW and IO+SW groups as compared to the CON group (11.7% and 15.9% respectively, both  $p < 0.05$ ), while no significant difference was observed between the IO and CON groups (Fig. 1). Also, the mean bodyweight in the IO+SW group was significantly lower than that in the SW group (13.0%,  $p < 0.05$ ). Initially, the approximate bodyweight of animals in the four groups was 220–235 g, but it increased to  $334 \pm 34$  g in the CON group before sacrifice. In contrast, bodyweight was  $323 \pm 19$  g,  $295 \pm 29$  g, and  $281 \pm 22$  g in the IO, SW, and IO+SW groups before sacrifice, respectively.

Various blood indexes were analyzed to obtain more information on the effect of the above mentioned different treatments on the rats. Results showed that, generally, there were significant differences in hemoglobin concentration [ $F(3, 36) = 12.061, p < 0.001$ ] and serum ferritin concentration [ $F(3, 36) = 10.621, p < 0.001$ ] among different groups (Table I). Compared with the CON group, hemoglobin concentration was significantly increased by 5.0% ( $p < 0.05$ ) and 5.7% ( $p < 0.05$ ) in the IO and IO+SW group, respectively, whereas no significant increase was observed with the SW group. At the same time, no

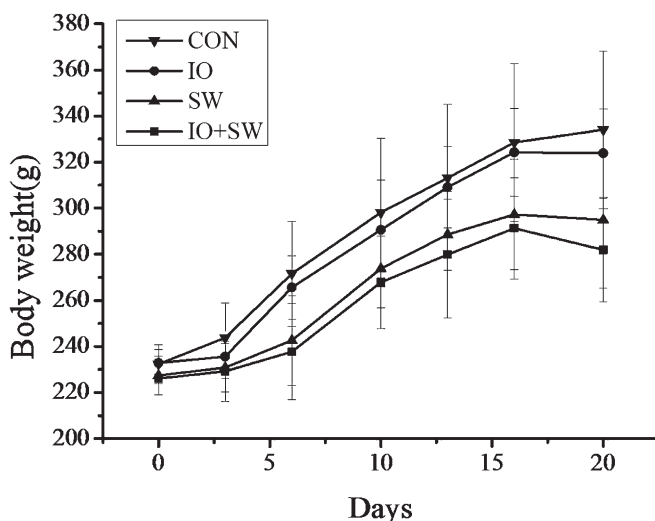


**Fig. 1.** Change in bodyweight of rats upon different treatments with iron overload (IO), simulated weightlessness (SW), and iron overload plus simulated weightlessness (IO+SW), respectively. Bodyweight was measured every 3 d. Data are expressed as means  $\pm$  SD

significant difference emerged between the IO and IO+SW group. Serum ferritin concentration was significantly increased by 71.7% ( $p < 0.05$ ) in the IO group as compared to the CON group, and it was 27.2% ( $p < 0.05$ ) above the IO value in the IO+SW group. However, the serum ferritin concentrations between the SW group and CON group were comparable. In contrast to the hemoglobin and serum ferritin concentrations, red blood cell numbers [ $F(3, 36) = 0.592, p = 0.624$ ] among the four groups were comparable.

According to the analysis of hematoxylin-eosin stained organ sections under a light microscope (Fig. 2; see online figure for color), no pathological change was discovered in the heart, kidney, musculus gastrocnemius, or duodenum sections (Fig. 2B, B5-B20) of all tested groups, whereas iron deposits (dark brown particles) can be clearly visualized in the liver (Fig. 2A, A2, A4) and spleen (Fig. 2B, B2, B4) of both the IO and IO+SW groups. Such deposition was more serious in the IO+SW group than the IO group. In the liver sections (Fig. 2A, A1-A4), the hepatocellular plates in the CON (Fig. 2A, A1) and SW (Fig. 2A, A3) groups were spokewheel-shaped, with the central vein as the center and distributed radially outward, with regularly scattered hepatic sinusoids. Compared to the CON and SW groups, the sections in the IO (Fig. 2A, A2) and IO+SW (Fig. 2A, A4) groups showed less regularity and more obvious iron deposition (dark brown particles). The same phenomenon and trend were discovered in the spleen sections, but not in the heart, kidney, musculus gastrocnemius, or duodenum sections.

To obtain more evidence for iron deposition in the liver, Prussian blue staining was used in the liver sections for the different groups (Fig. 2A, A5-A8). As expected, blue stained iron deposits can be observed in the cytoplasm of the hepatocytes in the IO (Fig. 2A, A6) and IO+SW groups (Fig. 2A, A8), and even were obviously denser in the IO+SW group, while no iron deposition was detected in the SW and CON groups.

In the micro-CT analysis (Fig. 3), it was observed that BV/TV [ $F(3, 36) = 14.090, p < 0.001$ ] was significantly reduced upon treatment with iron overload (10.9%,  $p < 0.01$ ), simulated weightlessness (18.8%,  $p < 0.01$ ), and their combination (15.6%,  $p < 0.01$ ) as compared to the CON group, respectively (Fig. 3A). The BV/TV in the IO+SW group was 5.3% lower than that of the IO group and 3.8% higher than that of the SW group, but there was no statistically significant difference among the three treated groups. Consistent with this conclusion, similar results were obtained in that thinner cortices and decreased cortical area are evident in the SW, IO, and IO+SW groups with respect to the control group (Fig. 3B).

To better understand the effect of the above mentioned different treatments on the rat femur, Tb.Th, Tb.N, and Tb.Sp in the different groups were further analyzed, and the results are shown in Table II. Generally, these parameters revealed a remarkable discrepancy between the different groups. As expected, Tb.Th [ $F(3, 36) = 9.161, p < 0.001$ ] was decreased in the IO, SW, and IO+SW groups by 9.3% ( $p < 0.05$ ), 28% ( $p < 0.05$ ), and 23% ( $p < 0.05$ ), respectively, as compared to the CON group. Compared to the IO group, Tb.Th was

**Table I.** Hemoglobin, Red Blood Cells, and Serum Ferritin in Each Experimental Group.

GROUP	CON	IO	SW	IO+SW
HGB (g/L)	168.50 ± 6.20	176.50 ± 8.91 <sup>a</sup>	167.63 ± 8.93	177.46 ± 10.37 <sup>a</sup>
RBC (×10 <sup>12</sup> /L)	7.64 ± 0.43	7.48 ± 0.54	7.42 ± 0.60	7.29 ± 0.53
FE (ng/mL)	37.12 ± 2.12	63.74 ± 6.60 <sup>a</sup>	44.88 ± 11.44	81.06 ± 7.78 <sup>b</sup>

HGB, hemoglobin and serum ferritin; RBC, number of red blood cells; FE, serum ferritin. Data are mean ± SD; <sup>a</sup>represents a significant difference from the CON group at  $p < 0.05$ ; <sup>b</sup>represents a significant difference from the IO group at  $p < 0.05$ .

statistically significantly lower ( $p < 0.05$ ) in the SW and IO+SW groups, but was comparable between the SW and IO+SW groups. Similarly, Tb.N [ $F(3, 36) = 10.097, p < 0.001$ ] was reduced in the IO, SW, and IO+SW groups by 10.4% ( $p < 0.05$ ), 26.2% ( $p < 0.05$ ), and 22.9% ( $p < 0.05$ ), respectively, as compared to the CON group. While the Tb.N in the SW and IO+SW groups was significantly lower ( $p < 0.05$ ) than that in the IO group, there was no significant difference between the

SW and IO+SW groups. In contrast to the trends in Tb.Th and Tb.N, Tb.Sp [ $F(3, 36) = 14.673, p < 0.001$ ] of the rat femur was increased with either iron overload or simulated weightlessness. Compared to the CON group, Tb.Sp was significantly increased by 27.9% ( $p < 0.05$ ), 42.3% ( $p < 0.05$ ), and 72.0% ( $p < 0.05$ ) in the IO, SW, and IO+SW groups, respectively. Meanwhile, the SW group exhibited significantly higher Tb.Sp than the IO group (2.6%,  $p < 0.05$ ), while the Tb.Sp in the IO+SW group (20.8%,  $p < 0.05$ ) was higher than that in the SW group.

To shed light on the effect caused by excessive iron in the combined model, we analyzed the relative concentration of hepcidin in the rat serum using Maldi-TOF MS, and the results are shown in Fig. 4. The serum hepcidin level [ $F(3, 36) = 85.119, p < 0.001$ ] of the rats increased in the IO and IO+SW groups by 117.5% ( $p < 0.01$ ) and 277.0% ( $p < 0.01$ ), respectively, as compared to the CON group, but no statistically significant difference in serum hepcidin level was observed between the CON and SW groups. Moreover, serum hepcidin level in the IO+SW group was significantly higher (73.3%,  $p < 0.01$ ) than that in the IO group.

## DISCUSSION

Iron overload and weightlessness might occur simultaneously during long-duration spaceflight. However, so far, there has been no information on their combined effect on animals or humans. The present studies demonstrate that the combination of iron overload and simulated weightlessness had significantly different effects on rats from that of iron overload or simulated weightlessness alone, and that these effects differed according to different organs.

Treatment with simulated weightlessness alone caused a significant reduction in rat body growth as compared with the CON group, while excessive iron did not result in a significant decrease in bodyweight growth (Fig. 1). Thus, under the present experimental conditions, a loss of bodyweight in the rats was mainly derived from the

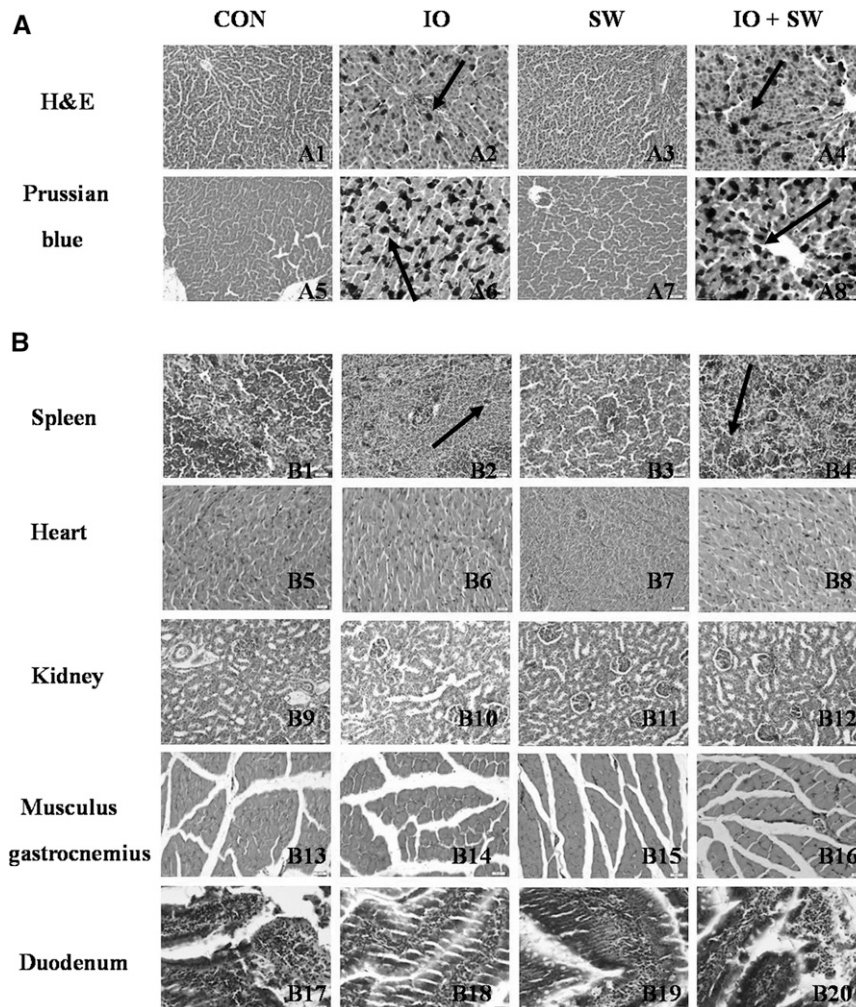


**Fig. 2.** Histological analyses of rats upon different treatments with iron overload (IO), simulated weightlessness (SW), and iron overload plus simulated weightlessness (IO+SW), respectively. Histological analysis of the sections from the liver (A1-8), spleen (B1-4), heart (B5-8), kidney (B9-12), musculus gastrocnemius (B13-16), and duodenum (B17-20) in each group are shown. Sections were submitted to hematoxylin and eosin (A1-4, B1-20) or Perl's Prussian blue (A5-8) and are shown at ×400 or ×200 magnification. Section A2, A4, B2, and B4 show hemosiderin deposition [brown arrows (see online figure for color)]; A6 and A8 show iron deposition [blue arrows (see online figure for color)].

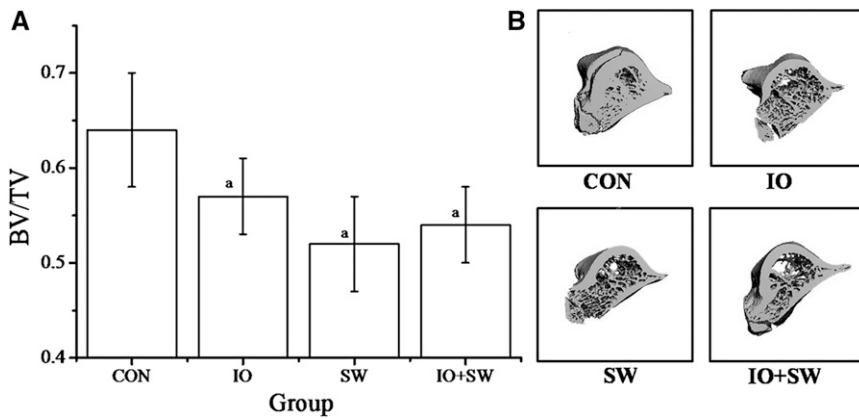


**Fig. 3.** Micro-CT analyses of rat femurs upon different treatments with iron overload (IO), simulated weightlessness (SW), and iron overload plus simulated weightlessness (IO+SW), respectively. A) Bone volume fractions (BV/TV) were represented in the histogram with SD. <sup>a</sup>*p* < 0.01 compared with the control (CON). B) Micro-CT images showing the thinning in the trabecular and cortical sections of the femur.

simulated weightlessness rather than the iron overload. This might be ascribed to the lower dosage of iron administration used in this study (total 500 mg · kg<sup>-1</sup>) as compared to the previous report (total 1496 mg · kg<sup>-1</sup>).<sup>14</sup> Consistent with the present observation, inhibition of bodyweight growth was likewise observed long before in the weightlessness model.<sup>17</sup> However, the presence of excessive iron aggravated the inhibition of the bodyweight growth of rats caused by simulated weightlessness (Fig. 1). A possible mechanism regarding this observation remains unknown.

Contrary to the above mentioned bodyweight results, the hemoglobin concentration of the SW group was nearly the same level as the CON group (Table I), indicating that treatment of rats with tail-suspension hardly affected hemoglobin concentration. Support for this idea comes from the observation that the hemoglobin concentration of the IO group was comparable with that of the IO+SW group. However, the hemoglobin concentration of both the IO+SW and IO groups was statistically significantly higher than that of the CON group (Table I), demonstrating that iron overload rather than hind limb unloading is a key factor which leads to an increase in the hemoglobin concentration of rats.

Serum ferritin has been widely used in clinical medicine to measure iron stores, which is considered as a good marker of iron level.<sup>6</sup> We successfully built an iron overload model with rats by the i.p. injection of iron-dextran based on the statistically higher level of serum ferritin in the IO group compared with the CON group (Table I). Consistent with the present

observation, previous studies also showed that serum ferritin level was also increased by excessive iron.<sup>6</sup> Interestingly, it was found in this study that a combination of iron overload and simulated weightlessness increased the ferritin level of the rats to a much higher level than iron overload or simulated weightlessness alone, suggesting that there is a synergistic effect between these two factors (iron overload or simulated weightlessness) on the above observed increase in the serum ferritin concentration of the rats. In contrast, the red blood cell numbers among the four groups were comparable (Table I), which is inconsistent with previous observation<sup>18</sup> of spaceflight from day 1 to day 120. The difference may due to a shorter period (only 24 d) applied in the present study as compared to the previous report.<sup>18</sup>

An obvious decrease in the regularity of cells and the deposition of iron in the liver sections in the IO and IO+SW groups compared with the CON and SW groups (Fig. 2A) confirmed the possibility that excessive iron in vivo might be consequently deposited into various parenchymal organs, especially in the liver, agreeing with previous observations.<sup>16</sup> Also, the more severe iron deposition in the liver sections in the IO+SW group compared with the IO group (Fig. 2A, A6, A8) indicated that the accumulation of excessive iron in the hepatic parenchymal cells is accelerated by simulated weightlessness, while simulated weightlessness alone cannot cause macroscopic iron deposition in the liver. Since the liver is mainly responsible for taking up and storing excessive amounts of iron, hepatotoxicity is the most consistent findings in patients suffering from iron overload and a similar iron deposition has been described along with some other liver injuries like fibrosis and, ultimately, cirrhosis.<sup>7</sup> The same phenomenon and trend were discovered in the spleen sections but not in the heart, kidney, musculus gastrocnemius, or duodenum sections (Fig. 2B). These results demonstrated that treatment with a combination of iron overload and simulated weightlessness synergistically caused the damage to the liver and spleen, consistent with the above serum ferritin concentration analyses as shown Table I.

Bone injury such as osteoporosis and fractures occurs frequently in disorders due to iron overload,<sup>21</sup> including thalassemias and hemochromatosis. It has been proposed that bone loss is associated with increased bone resorption,

**Table II.** Thickness, Number, and Spacing of Trabecula in the Femur.

GROUP	CON	IO	SW	IO+SW
Tb.Th (mm)	0.3870 ± 0.03	0.3509 ± 0.02 <sup>a</sup>	0.2784 ± 0.01 <sup>b</sup>	0.2968 ± 0.01 <sup>b</sup>
Tb.N (mm <sup>-1</sup> )	3.5783 ± 0.23	3.2076 ± 0.21 <sup>a</sup>	2.6425 ± 0.17 <sup>b</sup>	2.7602 ± 0.11 <sup>b</sup>
Tb.Sp (mm)	0.2225 ± 0.02	0.3087 ± 0.01 <sup>a</sup>	0.3167 ± 0.01 <sup>b</sup>	0.3827 ± 0.02 <sup>c</sup>

Tb.Th, trabecular thickness; Tb.N, trabecular number; Tb. Sp, trabecular spacing. Data are mean ± SD; <sup>a</sup>represents a significant difference from the CON group at *p* < 0.05; <sup>b</sup>represents a significant difference from the IO group at *p* < 0.05. <sup>c</sup>represents a significant difference from the SW group at *p* < 0.05.

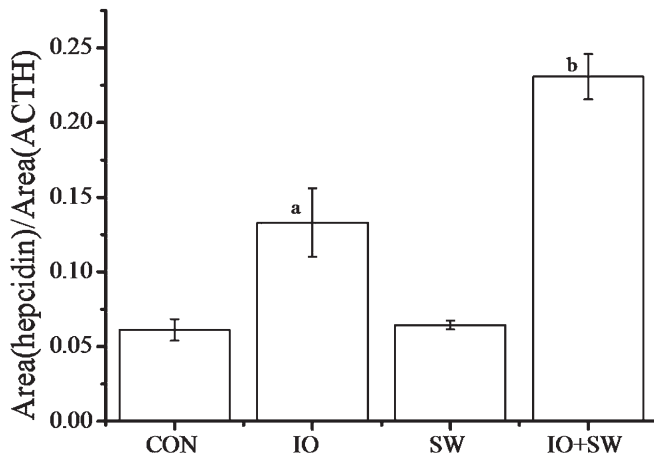


**Fig. 4.** Area under the curve resulting from analysis of hepcidin in the serum of rats upon different treatments with iron overload (IO), simulated weightlessness (SW), and iron overload plus simulated weightlessness (IO+SW), respectively. The histograms illustrate the peak area of hepcidin relative to that of ACTH (internal standard). Data represent the mean of 10 random samples in each group with SD. The peak area of each sample is an average which was taken from at least three independent analyses. <sup>a</sup> $p < 0.01$  compared with the SW and CON groups. <sup>b</sup> $p < 0.01$  compared with the IO group.

which is most probably related to the presence of increased ROS induced by excessive iron.<sup>20</sup> Indeed, the formation of bone and the differentiation of osteoblasts can be inhibited by exposure to excess iron ions.<sup>27</sup> On the other hand, bone loss is one of the changes with serious consequences, in particular for space travel of longer duration. Recent studies have shown that astronauts lost 1–2% bone weight per month during the course of the flight.<sup>11</sup> Consistent with previous studies,<sup>12, 20, 22</sup> treatment of rats with either iron overload or simulated weightlessness was found to cause the bone loss from the rat femur in this study (Fig. 3A). This result was in accordance with the fact that thinner cortices and decreased cortical area were found in the IO, SW, and IO+SW groups than the CON group (Fig. 3B). The bone volume fraction in the IO+SW group was lower than that of the IO group, but without significance, suggesting that simulated weightlessness does not facilitate the bone loss in iron-overloaded rats. This result is different from the above observation showing that treatment with iron overload plus simulated weightlessness has a more negative effect on the liver and spleen of rats (Fig. 2). Such a difference raises the possibility that the damage caused by a combination of iron overload and simulated weightlessness is organ-dependent.

A decrease in trabecular thickness and trabecular number was observed in the IO, SW, and IO+SW groups as compared with the CON group with a statistically significant difference (Table II). This decrease was significantly larger in the SW group than the IO group, while there was no statistical significance between the IO+SW and SW groups (Table 2). These results demonstrated that simulated weightlessness plays a more important role in bone loss as compared to iron overload

when rats were treated with iron overload and simulated weightlessness combined, and that the combined effect on the rat femur is not the simple addition of these two factors.

The absence of a statistically significant difference in hepcidin levels between the SW and CON groups (Fig. 4) indicated that simulated weightlessness alone did not cause the increase in hepcidin levels under the present experimental conditions. It has been established that hepcidin plays a key role in regulation of iron release from enterocytes of the proximal small intestine, macrophages, and monocytes. It performs the functions chiefly by altering the expression of ferroportin (Fpn) on the plasma membranes of these cells.<sup>5</sup> Specifically, when the circulating level of iron is high, the secretion of hepcidin will increase and lead to internalization of Fpn, thus decreasing iron transport out of enterocytes and macrophages. In contrast, when the level of iron is low, the secretion of hepcidin will decrease to ensure iron release from cells through Fpn.<sup>3</sup> Therefore, by modulating hepcidin production, organisms control intestinal iron absorption, iron uptake, and mobilization from stores to meet the body iron need. Thus, based on the present result (Fig. 4), it can be concluded that treatment with simulated weightlessness alone did not increase iron levels. In contrast, the statistically higher relative concentration of serum hepcidin was observed in the IO group compared to the CON group, indicating that treatment with iron overload caused the up-regulation of hepcidin in rats. Additionally, it was observed that the content of hepcidin was notably higher in the IO+SW group than that of the IO group, indicating that simulated weightlessness accelerated the up-regulation of hepcidin in rats caused by excessive iron. Thus, it appears that the combination of iron overload and simulated weightlessness has a synergistic effect on the increases of serum hepcidin in rats, as shown with the Prussian blue staining in the liver in Fig. 2.

Compared with the SW group, hepcidin level was significantly higher in the IO+SW group. Considering similar bone volume fractions observed in the two groups, we speculate that there might be an antagonistic effect between excessive iron and a high level of hepcidin caused by simulated weightlessness on bone growth of the femur of rats. Support for this idea came from previous studies that excessive iron can damage bone,<sup>10</sup> while hepcidin showed a positive effect on bone through increasing the calcification of human osteoblast cells.<sup>14</sup> Indeed, a recent study has reported that hepcidin increases intracellular  $\text{Ca}^{2+}$  of the osteoblast hFOB1.19 through L-type  $\text{Ca}^{2+}$  channels,<sup>26</sup> providing preliminary evidence that hepcidin could have an anti-osteoporosis effect. A detailed mechanism is under investigation.

In conclusion, we demonstrate for the first time that a combination of both iron overload and weightlessness simulated by tail-suspended hind limb unloading has a pronouncedly distinct effect on rats compared with each factor alone. In this combined model, iron overload rather than simulated weightlessness played a much more important role in the increase in hemoglobin and serum ferritin concentration, and iron deposition in the liver and spleen of rats, but simulated weightlessness facilitated the increase and iron deposition, indicative of

a synergistic effect between these two factors. In contrast, simulated weightlessness appears to be mainly responsible for the damage to the femur of rats, while treatment with iron overload somehow alleviated such damage, demonstrating an antagonistic effect between these two factors occurring on the rat femur.

## ACKNOWLEDGMENTS

This project was supported by the National Natural Science Foundation of China (31271826) and the National Science and Technology Support Program (2011BAD23B04).

*Authors and affiliations:* Aidong Wang, B.Sc., Jiachen Zang, M.Eng., B.Eng., and Guanghua Zhao, Ph.D., M.Sc., CAU & ACC Joint Laboratory of Space Food, College of Food Science and Nutritional Engineering, China Agricultural University, Beijing, China; Jing Wang, M.Sc., B.Sc., and Guangjun Nie, Ph.D., M.Sc., Chinese Academy of Sciences Key Laboratory for Biomedical Effect of Nanomaterials and Nanosafety, National Center for Nanosciences and Technology of China, Beijing, China; and Bin Chen, Ph.D., M.Eng., Key Laboratory of Space Nutrition and Food Engineering, China Astronaut Research and Training Center, Beijing, China.

## REFERENCES

- Aguirre JI, Plotkin LI, Stewart SA, Weinstein RS, Parfitt AM, et al. Osteocyte apoptosis is induced by weightlessness in mice and precedes osteoclast recruitment and bone loss. *J Bone Miner Res.* 2006; 21(4):605–615.
- Basso N, Bellows CG, Heersche JNM. Effect of simulated weightlessness on osteoprogenitor cell number and proliferation in young and adult rats. *Bone.* 2005; 36(1):173–183.
- Camberlein E, Abgueguen E, Fatih N, Canonne-Hergaux F, Leroyer P, et al. Hepcidin induction limits mobilisation of splenic iron in a mouse model of secondary iron overload. *Biochim Biophys Acta.* 2010; 1802(3):339–346.
- Fan J, Niu S, Dong A, Shi J, Wu HJ, et al. Nanopore film based enrichment and quantification of low abundance hepcidin from human bodily fluids. *Nanomedicine.* 2014; 10(5):879–888.
- Ganz T. Iron homeostasis: fitting the puzzle pieces together. *Cell Metab.* 2008; 7(4):288–290.
- García-Yébenes I, Sobrado M, Moraga A, Zarruk JG, Romera VG, et al. Iron overload, measured as serum ferritin, increases brain damage induced by focal ischemia and early reperfusion. *Neurochem Int.* 2012; 61(8):1364–1369.
- Gao Y, Wang N, Zhang Y, Ma Z, Guan P, et al. Mechanism of protective effects of Danshen against iron overload-induced injury in mice. *J Ethnopharmacol.* 2013; 145(1):254–260.
- Halliwel B, Gutteridge J. Oxygen toxicity, oxygen radicals, transition metals and disease. *Biochem J.* 1984; 219(1):1–14.
- Hentze MW, Muckenthaler MU, Galy B, Camaschella C. Two to tango: regulation of Mammalian iron metabolism. *Cell.* 2010; 142(1):24–38.
- Kudo H, Suzuki S, Watanabe A, Kikuchi H, Sassa S, Sakamoto S. Effects of colloidal iron overload on renal and hepatic siderosis and the femur in male rats. *Toxicology.* 2008; 246(2-3):143–147.
- Kondo H, Yumoto K, Alwood JS, Mojarrab R, Wang A, et al. Oxidative stress and gamma radiation-induced cancellous bone loss with musculoskeletal disease. *J Appl Physiol.* 2010; 108(1):152–161.
- Lloyd SA, Bandstra ER, Willey JS, Riffle SE, Tirado-Lee L, et al. Effect of proton irradiation followed by hindlimb unloading on bone in mature mice: a model of long-duration spaceflight. *Bone.* 2012; 51(4):756–764.
- Morey-Holton ER, Globus RK. Hindlimb unloading rodent model: technical aspects. *J Appl Physiol.* 2002; 92(4):1367–1377.
- Mandalunis P, Gibaja F, Ubios AM. Experimental renal failure and iron overload: A histomorphometric study in the alveolar bone of rats. *Exp Toxicol Pathol.* 2002; 54:85–90.
- Nemeth E, Tuttle MS, Powelson J, Vaughn MB, Donovan A, et al. Hepcidin regulates cellular iron efflux by binding to ferroportin and inducing its internalization. *Science.* 2004; 306(5704):2090–2093.
- Puntarulo S. Iron, oxidative stress and human health. *Mol Aspects Med.* 2005; 26(4-5):299–312.
- Royland JE, Weber LJ, Fitzpatrick M. Testes size and testosterone levels in a model for weightlessness. *Life Sci.* 1994; 54(8):545–554.
- Smith SM. Red blood cell and iron metabolism during space flight. *Nutrition.* 2002; 18(10):864–866.
- Steenma DP, Gattermann N. When is iron overload deleterious, and when and how should iron chelation therapy be administered in myelodysplastic syndromes? *Best Pract Res Clin Haematol.* 2013; 26:431–444.
- Tsay J, Yang Z, Ross FP, Cunningham-Rundles S, Lin H, et al. Bone loss caused by iron overload in a murine model: importance of oxidative stress. *Blood.* 2010; 116(14):2582–2589.
- Vogiatzi MG, Macklin EA, Fung EB, Cheung AM, Vichinsky E, et al. Bone disease in thalassemia: a frequent and still unresolved problem. *J Bone Miner Res.* 2009; 24(3):543–557.
- Valenti L, Varenna M, Fracanzani AL, Rossi V, Fargion S, Sinigaglia L. Association between iron overload and osteoporosis in patients with hereditary hemochromatosis. *Osteoporos Int.* 2009; 20(4):549–555.
- Wang X, Guo B, Li Q, Peng J, Yang Z, et al. miR-214 targets ATF4 to inhibit bone formation. *Nat Med.* 2013; 19(1):93–100.
- Ward DM, Kaplan J. Ferroportin-mediated iron transport: expression and regulation. *Biochim Biophys Acta.* 2012; 1823(9):1426–1433.
- Ware RE, Zimmerman SA, Sylvestre PB, Mortier NA, Davis JS, et al. Prevention of secondary stroke and resolution of transfusional iron overload in children with sickle cell anemia using hydroxyurea and phlebotomy. *J Pediatr.* 2004; 145(3):346–352.
- Xu Y, Li G, Du B, Zhang P, Xiao L, et al. Hepcidin increases intracellular Ca<sup>2+</sup> of osteoblast hFOB1.19 through L-type Ca<sup>2+</sup> channels. *Regul Pept.* 2011; 172(1-3):58–61.
- Yamasaki K, Hagiwara H. Excess iron inhibits osteoblast metabolism. *Toxicol Lett.* 2009; 191(2-3):211–215.